5600 *Macromolecules* **2009**, *42*, 5600–5604
DOI: 10.1021/ma900761w

Macromolecules
ARTICLE

Electromechanics of Monodomain Chiral Smectic C Elastomer: Mechanical Response to Electric Stimulation

Kazuyuki Hiraoka,*,† Manami Kobayasi,† Ryugo Kazama,† and Heino Finkelmann‡

†*Center for Nano Science and Technology, Department of Life Science & Sustainable Chemistry, Tokyo Polytechnic University, 1583 Iiyama, Atsugi-shi 243-0297, Japan, and* ‡*Institut für Makromolekulare Chemie, Albert-Ludwigs-Universität Freiburg, Stefan-Meier-Strasse 31, D-79104 Freiburg i. Br., Germany*

Received April 15, 2009; Revised Manuscript Received June 24, 2009

Introduction

Liquid crystalline elastomers have been paid increasing attention as a novel class of liquid crystalline materials because they give rise to new macroscopic features by combining the mechanical properties of polymer network with the anisotropic structure of liquid crystalline phases.[1−9] In particular, smectic C (SmC) elastomers composed of chiral mesogens have attracted interest in both industrial and scientific fields, because of their additional properties such as piezoelectricity, ferroelectricity, pyroelectricity and second harmonic generation (SHG), which result from the symmetry breaking brought by the molecular chirality.[10−18] It is worth mentioning that they are ideal materials for the investigation of piezoelectric and inverse piezoelectric effects in chiral smectic C (SmC*) systems, because polymer network prevents macroscopic flow, which disturbs the emergence of piezoelectricity in conventional low-molar mass ferroelectric liquid crystals.[19−28] To date, several groups have demonstrated electric-field-induced deformation due to the inverse piezoelectric effect in chiral smectic elastomers, focusing on their potential applications as electrically controllable soft actuators.[26−30] Lehmann et al.[26] and Köhler et al.[27] verified the film thickness variation that was induced by the electroclinic response in a freely suspended film composed of a chiral smectic elastomer. Moreover, Spillmann et al. observed anisotropic electrostriction in chiral liquid-crystalline elastomers, that displayed planar textures which corresponded to the smectic A phase with good director alignment.[28] Adams and Warner theoretically described SmC elasticity and mechanical switching of the polarization in the chiral system.[29,30] In addition, Stenull et al. predicted a shear induced tilt in SmA elastomers,[31] and Kramer et al. confirmed it by means of X-ray experiments under shear strain.[32]

Despite these studies reported so far, the details of the piezoelectric and inverse piezoelectric properties of chiral smectic elastomers are still unknown because of the lack of a monodomain sample. We have recently succeeded in obtaining monodomain SmC* elastomers with macroscopic C_2 symmetry of the unwound SmC* state by biaxial mechanical deformation, such as two successive deformation processes and more perfectly mechanical shear deformation.[13,15] Moreover, we confirmed that these samples exhibit a biaxial shape change under thermal stimulation, which is spontaneous and reversible shear deformation in a heating and cooling process where successive phase transitions take place.[16] The purpose of this paper is to show a macroscopic mechanical response to the electric excitation of the monodomain SmC* elastomers obtained by the shear deformation. We observe that shrinkage and elongation in the direction of the layer normal takes place upon application of an electric field parallel to the layers. The magnitude of the electric-field-induced deformation attains a maximum in the vicinity of the SmA-to-SmC* transition temperature, because it is associated with the critical behavior of the electroclinic effect described as the fluctuation of the molecular tilt angle with respect to the layer normal.[33,34]

*Author for correspondence. Telephone: +81-46-242-9526. Fax: +81-46-242-3000. E-mail: hiraoka@nano.t-kougei.ac.jp.

Experimental Section

An elastomer is synthesized by the hydro-silylation reaction of the liquid-crystalline side groups with a polysiloxane backbone according to the well-known synthesis route.[1] The chemical structures of the polymer backbone, the mesogens and the cross-linker are shown in Figure 1. The elastomer contains two different mesogenic moieties statistically linked to the monomer units of the network and shows the following phase sequence:

$$\text{g } -6 \text{ SmX* (SmF*) } 32 \text{ SmC* } 80 \text{ SmA } 115 \text{ I} \quad \text{(in °C)}$$

The transition temperatures listed above are determined by DSC measurement and X-ray scattering observation, as already reported in previous papers.[15,16] Because the X-ray pattern revealed that the SmX* phase is one of the high-ordered tilted smectic phases, it may be tentatively assigned to SmF* here.

The elastomer film is prepared by the spin-casting technique in solution, which contains the polysiloxane (2 mmol), mesogen A (1.2 mmol), mesogen B (0.4 mmol), the cross-linker (0.2 mmol), and 6 μL of the Pt-catalyst SLM86005 (Wacker Chemie, Burghausen, Germany) in 2 mL of toluene. The reaction is carried out under centrifugation (3000 rpm) at 90 °C for 2 h. Thereafter, the reaction vessel is cooled to room temperature and the elastomer, swollen with toluene, is carefully removed from the vessel. In order to obtain a uniform orientation of director, the swollen elastomer is deformed uniaxially by loading it with a stress of 25 mN/mm^2 for 1 h. After the uniaxial deformation, the elastomer is fixed onto a simple shear apparatus and gradually sheared with an angle θ of $\sim 20°$ at room temperature (25 °C), as shown in Figure 2. The elastomer is kept under mechanical shear field for about 3 h until the cross-linking reaction is completed. During these deformation processes at room temperature, the toluene evaporates continuously from the network and the successive phase transformations occur from the isotropic phase of the gel to the tilted smectic phase of the dry network. In addition, the sample is annealed within the SmC* phase at 60 °C for about 1 h to accelerate the reorientation process. Finally, a monodomain sample of the smectic C elastomer whose X-ray photograph is shown in Figure 3(a) was obtained.

The alignment of the elastomer is observed by X-ray measurements with a rotating anode X-ray system. The measurements are

 Published on Web 07/08/2009

mainly performed using a Cu Kα beam filtered by a confocal mirror (wavelength = 1.54 Å, X-ray power = 2.7 kW) and a two-dimensional image plate system (2540 × 2540 pixels, 50 μm resolution). The distance between the sample and the image plate is 100 mm.

The electric-field-induced deformation is observed using a CCD camera attached to a microscope under an electric field E, which is applied parallel to the smectic layer. The electric field of up to 2.5 V/μm is applied using a function generator (NF, Wave factory 1941) and an operational amplifier (NF, AC/DC amplifier HVA4321). Electrode layers of silver conductive grease (Circuit Works) are coated on either side of the elastomer whose thickness is about 400 μm. The area of the electrode is about 2-mm-square. The film of the SmC* elastomer is mounted in a laboratory-made furnace connected to a temperature regulator (Chino, model DB1000) during the sample observation.

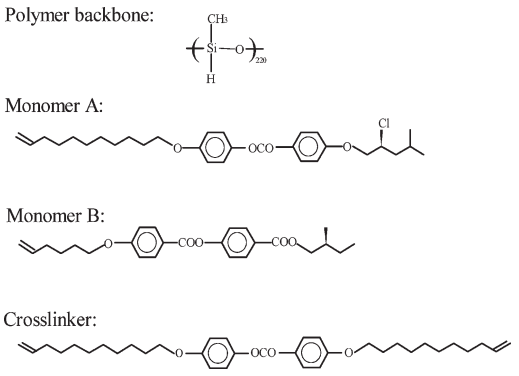

Figure 1. System for investigation.

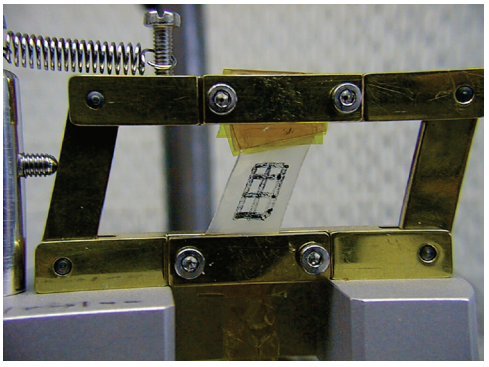

Figure 2. Cross-linking reaction under mechanical shear field.

Results and Discussion

An X-ray scattering pattern of the sample, which is set up for observing electric-field-induced deformation, is shown in Figure 3a. It was taken in the SmC* phase at 35 °C. The X-ray pattern discloses that both the mesogens and layers are uniformly aligned. While the layer reflection located near the meridian (arrow 1) indicates a uniform alignment of smectic layers in the tilted smectic phase, the reflection at a wide angle (arrow 2) indicates that the mesogenic groups are aligned uniformly in the direction inclined as θ_X with respect to the layer normal. On the basis of the X-ray pattern, we depict the molecular orientation within the sample setup for the observation in Figure 3b. Here, the topside of the elastomer is fixed to a sample holder, while the lower end can move freely so as not to disturb the electric-field-induced deformation. Additionally, a micrograph of the elastomer is shown in Figure 3c, which is an enlarged image of the square section within the dotted line in Figure 3b. Although the upper part of the elastomer in Figure 3c is not transmissive because of the silver grease coated as electrodes, the elastomer near the lower end is brighter because no grease is coated to avoid electric discharge.

We estimate the electric-field-induced deformation $\Delta L = L_{(E)} - L_{(0)}$, which is defined as shrinkage and/or elongation in the direction of the layer normal, as shown in Figure 3b. $L_{(E)}$ is the sample length under an electric field E. Here, an electric field applied parallel to the y-direction in Figure 3 is tentatively defined as "a positive electric field". To investigate the mechanical response to electric stimulation in the chiral smectic system, ΔL is plotted as a function of electric field strength in Figure 4, which is obtained just above the SmC*-to-SmA phase transition temperature at 80 °C. The elastomer shrinks upon application of the positive electric field, as shown in Figure 4, where ΔL decreases with increasing field strength and reaches about −5 μm under an electric field of +2.5 V/μm. On the other hand, the elastomer elongates upon application of the negative field, that is, the electric field in the opposite direction; ΔL is estimated to be about +3.5 μm under an electric field of −2.5 V/μm. Because not dielectric anisotropy but polarization is related to the deformation, the direction of deformation, namely, whether shrinkage or

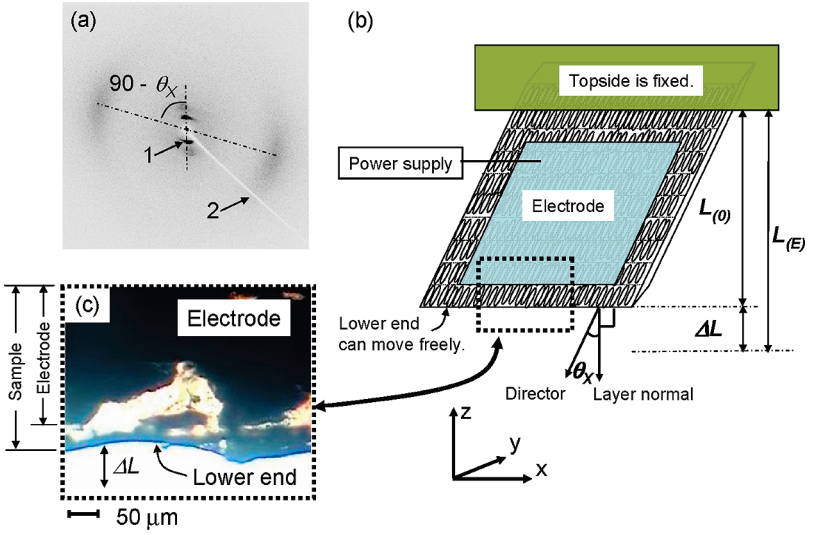

Figure 3. Sample for observation of electric-field-induced deformation: (a) X-ray scattering pattern in the SmC* phase at 35 °C, (b) its molecular alignment, and (c) micrograph image corresponding to square section within dotted line in part b.

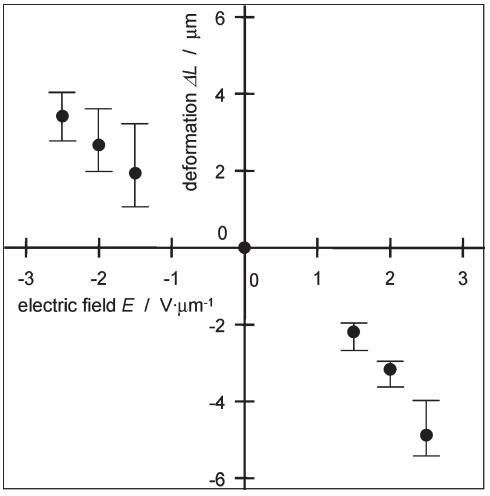

Figure 4. Relationship between electric field E and field-induced deformation in the direction of layer normal ΔL.

elongation occurs, depends on the polarity of the applied electric field. In other words, coupling between the polarization and the electric field contributes to the electric-field-induced deformation in the monodomain chiral smectic elastomer.

To consider the electric-field-induced deformation from a molecular point of view, the molecular tilt angle θ_X, which is estimated by means of X-ray measurement (see Figure 3a and Figure 3b), is plotted as a function of temperature in Figure 5a. The value of θ_X, which is about 27° at room temperature (25 °C), decreases with increasing temperature in the tilted smectic phases such as SmF* and SmC* until the SmC*-to-SmA transition temperature at about 80 °C. For a further increase in temperature in the SmA phase, θ_X remains at about 5° because of the residual SmC* order fixed by cross-linking. This implies that an internal mechanical shear stress within the cross-linked system induces the residual tilt angle in the temperature region of SmA.[31,32,35] The temperature dependence of θ_X shows that the measurement of the field-induced deformation in Figure 4 was carried out just above the SmC*-to-SmA phase transition temperature, where a pretransitional phenomenon such as the electroclinic effect should emerge. Accordingly, we may say that the deformation of the elastomer is caused by the electroclinic effect, which stands for the direct coupling of the molecular tilt angle θ_X to the applied electric field E.[33,34]

To understand the mechanism of the electric-field-induced deformation, we illustrate a schematic model describing the electroclinic response in the SmA temperature region where the residual tilt angle remains at several degrees because of cross-links (Figure 6b). Since θ_X is related to the tilted layer spacing d and the nontilted layer spacing d_A in the following equation,[36]

$$d = d_A \cos \theta_X \quad (1)$$

the increase (decrease) in θ_X corresponds to the decrease (increase) in the layer spacing d. The residual-tilted structure causes a polarization (tentatively designated as "a residual polarization") with no electric field because of symmetry breaking in the chiral smectic A system.[37] Since the tilt angle θ_X increases upon application of an electric field parallel to the residual polarization because of the electroclinic response, the decrease in the layer spacing d simultaneously occurs, as illustrated in Figure 6a. Here, the field parallel to the residual polarization corresponds to "a positive field" in the description of Figure 4. In addition, the elastomer elongates upon application of an electric field antiparallel to the residual polarization, because both the decrease in θ_X and the increase in d take place together (Figure 6c). Accordingly, the field-induced deformation

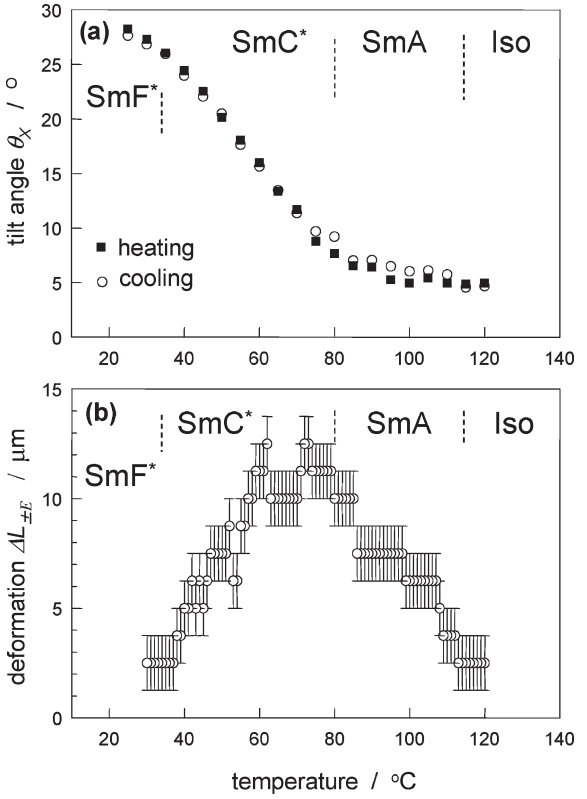

Figure 5. Temperature dependence of (a) molecular tilt angle θ_X and (b) electric-field-induced deformation $\Delta L_{\pm E}$ under a 0.5-Hz rectangular electric wave of ±2.5 V/μm.

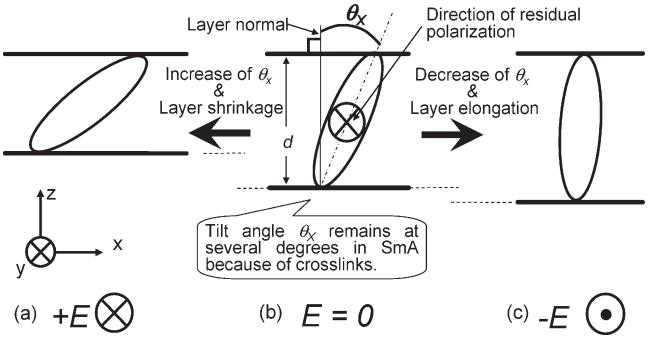

Figure 6. Schematic model describing electroclinic response in the SmA region where a residual tilt angle remains because of cross-links: (a) under $-E$, (b) $E = 0$, and (c) under $+E$.

of the elastomer can be explained by the change of d caused by the electroclinic response within the residual-tilted structure in the SmA region, because the sample length L is directly coupled with the layer spacing d.

Additionally, let us consider the influence of the internal mechanical stress, which induces the residual tilt angle in the SmA phase, on the relationship between E and ΔL depicted in Figure 4.[35] Since the internal stress may enhance (disturb) tilting in its own (opposite) direction, the relationship between E and ΔL becomes asymmetric with respect to the interchange of positive and negative electric fields. In other words, the asymmetric relationship indicates that the elastomer has a preferable tilt direction originated by the internal mechanical stress which induces the residual tilt angle. In addition, the relationship seems to be nonlinear especially in the positive field. However, to discuss the nonlinearity is beyond the scope of this paper. In the meantime, we proceed to estimate the induced tilt angle for further discussion.

To investigate the critical behavior of the electroclinic effect, we carried out a further experiment on the temperature dependence of the electric-field-induced deformation. Here, we estimate the deformation $\Delta L_{\pm E} = L_{(-E)} - L_{(+E)}$ observed under a 0.5-Hz rectangular electric wave of ± 2.5 V/μm. $\Delta L_{\pm E}$ is plotted as a function of temperature in Figure 5b. A small deformation at about $\Delta L_{\pm E} = 2$ μm is recognized in the vicinity of the SmA-to-Iso phase transition temperature, where the smectic structure may partially remain because of cross-links. The value of $\Delta L_{\pm E}$ increases with decreasing temperature in the temperature region of the smectic A phase and reaches a maximum value of 12 μm at about the SmA-to-SmC* phase transition temperature, where the softening of the collective fluctuation of θ_X takes place because of the critical behavior of the electroclinic effect.[34] The value of $\Delta L_{\pm E}$ seems to keep at about 10−12 μm during a part of the SmC* temperature region between 80 and 60 °C. One may notice that not only the soft mode corresponding to the electroclinic effect but also the Goldstone mode describing the fluctuation of the azimuthal angle is excited by the electric field in SmC* systems.[38] However, the Goldstone mode does not contribute effectively to the sample deformation, because the layer spacing d does not change with the fluctuation of the azimuthal angle. In addition, the internal mechanical stress, which induces the residual tilt angle in SmA, may suppress the Goldstone mode in the SmC* phase where the helix is unwound in the monodomain SmC* elastomer. Therefore, the origin of the electric-field-induced deformation observed in the SmC* phase of the elastomer may be mainly attributed to the contribution of the soft mode due to the electroclinic response. To estimate quantitatively the contribution of the Goldstone and soft modes in the SmC* phase, a tensor analysis of the mechanical response should be carried out as a next step.[39] For a further decrease in temperature in the SmC* region, $\Delta L_{\pm E}$ decreases to 2 μm at 40 °C where the SmC*-to-SmF* phase transition takes place. Additionally, a small deformation of about $\Delta L_{\pm E} = 2$ μm is observed in the temperature range of the SmF* phase.

Let us compare our results to those in the previous study by Lehmann et al.[26] They reported that the thickness change Δh, namely, the shrinkage parallel to the layer normal, was electrically induced in homeotropically aligned SmC* elastomers. According to their estimation, Δh was less than 10 nm under 1.5 V/μm, and it corresponded to the 4% strain of the sample thickness. As already mentioned above, the induced deformation $\Delta L_{\pm E}$ attains to 12 μm in our experiment. The value of $\Delta L_{\pm E}$ (12 μm) is more than 1000 times that of Δh reported by Lehmann et al. On the other hand, however, the strain ($\Delta L_{\pm E}/L \times 100$ (%)) is estimated at only about 0.6% in our case, while Lehmann's Δh reaches 4%. Because the electrode is not coated near the edge of our elastomer to avoid electric discharge (see Figure 3c), the edge part may disturb the deformation of the elastomer as a whole. Accordingly, such a small strain, only 0.6%, is apparently observed in our experiments. Nevertheless, the electrically driven deformation parallel to the layer normal in the SmC* elastomers is definitely interesting for industrial application as soft actuator and/or artificial muscle, because the high-performance mechanical properties attributable to the one-dimensional crystalline structure, such as high modulus, etc., are expected in smectic elastomers.[40]

Although the electric-field-induced deformation has been recognized for a wide temperature range between the isotropic phase and the SmF* phase, we have tentatively concluded that the deformation is caused by the electroclinic effect. In general, however, the electroclinic effect is exhibited in a narrow temperature range near the SmA-to-SmC* phase transition temperature, because it is one of the pretransitional phenomena. This contradiction suggests that polymer network affects the critical behavior of the electroclinic response in the chiral smectic system. At present, we speculate that the SmC*-to-SmA transition temperature is distributed by the formation of polymer network, which broadens the SmC*-to-SmA transformation range. In addition, the influence of the internal mechanical stress on the SmC*-to-SmA transformation should be examined for further discussion about the temperature dependence of the electrically induced deformation of the monodomain SmC* elastomer. In the meantime, we try to measure the change of the optical axis under an electric wave to discuss quantitatively the mechanical response to electric stimulation in chiral smectic elastomers. We hope to elucidate a number of electromechanic questions and to confirm our hypothesis by showing experimental details in the near future.

Conclusion

We have investigated the mechanical response to electric stimulation in a monodomain chiral smectic C elastomer. The electric-field-induced deformation, such as shrinkage and elongation parallel to the layer normal, was observed in the chiral smectic phases appearing in the successive phase transformations. Because polarization, and not dielectric anisotropy, was closely associated with the electric-field-induced deformation, the direction of deformation, namely, shrinkage or elongation, depended on the polarity of the applied electric field. Additionally, we tentatively concluded that the electroclinic effect, i.e., the direct coupling of the molecular tilt angle to the applied electric field, caused the electric-field-induced deformation whose magnitude attained a maximum in the vicinity of the SmA-to-SmC* transition temperature because of its critical behavior. In addition, we suggest that the polymer network may affect the critical behavior of the electroclinic effect in chiral smectic elastomers.

Acknowledgment. We are grateful to Mr. Tohru Tashiro for his experimental assistance. K.H. thanks Professor Masanori Ozaki (Osaka University) and Professor Hideo Takezoe (Tokyo Tech.) for their valuable comments. This work was supported by a Grant-in-Aid for Scientific Research (C) (No. 20550167) from the Ministry of Education, Culture, Sports, Science, and Technology (MEXT) and was partially supported by the Deutsche Forschungsgemainshaft, SFB 428.

References and Notes

(1) Finkelmann, H.; Kock, H. J.; Rehage, G. *Makromol. Chem., Rapid Commun.* **1981**, *2*, 317.
(2) Zentel, R.; Reckert, G. *Makromol. Chem.* **1986**, *187*, 1915.
(3) Mitchell, G. R.; Davis, F. J.; Ashman, A. *Polymer* **1987**, *28*, 639.
(4) Brand, H. R.; Finkelmann, H.; *Handbook of Liquid Crystals*, Demus, D., Goodby, J., Gray, G. W., Spiess, H.-W., Vill, V., Eds.; Wiley-VCH: Weinheim, Germany, 1998; *Vol. 3*, pp 277−302.
(5) Zentel, R. *Angew. Chem. Adv. Mater.* **1989**, *101*, 1437.
(6) Davis, F. J. *J. Mater. Chem.* **1993**, *3*, 551.
(7) Warner, M.; Terentjev, E. M.; *Liquid Crystal Elastomers*; Clarendon Press: Oxford, U.K., 2003; pp 1−7 and pp 93−106.
(8) Yusuf, Y.; Huh, J.-H.; Cladis, P. E.; Brand, H. R.; Finkelmann, H.; Kai, S. *Phys. Rev. E* **2005**, *71*, 061702.
(9) Urayama, K. *Macromolecules* **2007**, *40*, 2277.
(10) Terentjev, E. M.; Warner, M. *J. Phys. II Fr.* **1994**, *4*, 849.
(11) Brehmer, M.; Zentel, R.; Wagenblast, G.; Siemensmeyer, K. *Macromol. Chem. Phys.* **1994**, *195*, 1891.
(12) Benné, I.; Semmler, K.; Finkelmann, H. *Macromol. Rapid Commun.* **1994**, *15*, 295.
(13) Semmler, K.; Finkelmann, H. *Macromol. Chem. Phys.* **1995**, *196*, 3197.
(14) Eckert, T.; Finkelmann, H.; Keck, M.; Lehmann, W.; Kremer, F. *Macromol. Rapid Commun.* **1996**, *17*, 767.
(15) Hiraoka, K.; Finkelmann, H. *Macromol. Rapid Commun.* **2001**, *22*, 456.
(16) Hiraoka, K.; Sagano, W.; Nose, T.; Finkelmann, H. *Macromolecules* **2005**, *38*, 7352.
(17) Stenull, O.; Lubensky, T. C. *Phys. Rev. Lett.* **2005**, *94*, 018304.
(18) Adams, J. M.; Warner, M. *Phys. Rev. E* **2006**, *73*, 031706.

(19) Zentel, R. *Liq. Cryst.* **1988**, *3*, 531.
(20) Brand, H. *Makromol. Chem., Rapid Commun.* **1989**, *10*, 441.
(21) Vallerien, S. U.; Kremer, F.; Fischer, E. W.; Kapitza, H.; Zentel, R.; Poths, H. *Makromol. Chem., Rapid Commun.* **1990**, *11*, 593.
(22) Meier, W.; Finkelmann, H. *Macromolecules* **1993**, *26*, 1811.
(23) Mauzac, M.; Nguyen, H.-T.; Tournilhac, F.-G.; Yablonsky, S.-V. *Chem. Phys. Lett.* **1995**, *240*, 461.
(24) Lehmann, W.; Leister, N.; Hartmann, L.; Geschke, D.; Kremer, F.; Stein, P.; Finkelmann, H. *Mol. Cryst. Liq. Cryst.* **1999**, *328*, 437.
(25) Hiraoka, K.; Stein, P.; Finkelmann, H. *Macromol. Chem. Phys.* **2004**, *205*, 48.
(26) Lehmann, W.; Skulpin, H.; Tolksdorf, C.; Gebhard, E.; Zentel, R.; Krüger, P.; Lösche, M.; Kremer, F. *Nature* **2001**, *410*, 447.
(27) Köhler, R.; Stannarius, R.; Tolksdorf, C.; Zentel, R. *Appl. Phys. A: Mater. Sci. Process.* **2005**, *80*, 381.
(28) Spillmann, C. M.; Ratna, B. R.; Naciri, J. *Appl. Phys. Lett.* **2007**, *90*, 021911.
(29) Adams, J. M.; Warner, M. *Phys. Rev. E* **2008**, *77*, 021702.
(30) Adams, J. M.; Warner, M. *Condensed Matter* **2008**, *0812*, 1746.
(31) Stenull, O; Lubensky, T. C.; Adams, J. M.; Warner, M. *Phys. Rev. E* **2008**, *78*, 021705.
(32) Kramer, D; Finkelmann, H *Phys. Rev. E* **2008**, *78*, 021704.
(33) Garoff, S; Meyer, R. B. *Phys. Rev. A* **1979**, *19*, 338.
(34) Bahr, C. H.; Heppke, G. *Liq. Cryst.* **1987**, *2*, 825.
(35) Brehmer, M.; Zentel, R.; Giesselmann, F.; Germer, R.; Zugenmaier, P *Liq. Cryst.* **1996**, *21*, 589.
(36) Vries A. de *Mol. Cryst. Liq. Cryst.* **1970**, *10*, 219.
(37) Meyer, R. B.; Liébert, L.; Strzelecki, L.; Keller, P. *J. Phys.* (*Paris*), *Lett.* **1975**, *36*, L69.
(38) Blinc, R.; Zěkš, B. *Phys. Rev. A* **1978**, *18*, 740–745.
(39) Kubota, S. Masters Thesis, Hokkaido University, Sapporo, Japan, 2009.
(40) Nishikawa, E.; Finkelmann, H. *Macromol. Rapid Commun.* **1997**, *18*, 65.